Systems and Computers in Japan, Vol. 22, No. 11, 1991
Translated from Denshi Joho Tsushin Gakkai Ronbunshi, Vol. 73-DII, No. 12, December 1990, pp. 1993-2000

Extraction of Surface Orientation from Texture Using the Gray Level Difference Statistics

Hidegi Matsushima, Nonmember, Mutsuhiro Terauchi, Toshio Tsuji, and Koji Ito, Members

Faculty of Engineering, Hiroshima University, Higashi-Hiroshima, Japan 724

SUMMARY

The problem of extracting orientation of an object surface from a monocular image is one of the important tasks in computer vision. Most of the existing methods for extracting surface orientation are ones using the structural features of texture such as texel and edge. However, to represent texture features statistically is shown to be effective also in texture discrimination and segmentation. Thus, in this paper we propose a method for extracting surface orientation using the statistical feature of a texture image.

First, we assume uniformity of a probability density function of difference statistic on object surface; then using the fact that the difference statistics depend on the geometric factor of length and orientation, we formulate the relationship between distortion of a density function in an image caused by perspective projection and the object surface. Then we derive an algorithm for finding the object surface orientation by search based on this formulation. In addition we apply this method to simulation images and real images to show its effectiveness. This enables us to extract object surface directly from a gray level image without extracting the texel or edge (whose extraction is required in the existing methods).

1. Introduction

The problem of reconstructing a 3-D world from a 2-D image is one of the important themes of computer vision. In this paper we consider the problem of extracting object surface orientation from a monocular view image, which is one of important steps in reconstructing a 3-D structure. This problem becomes an ill-posed problem since information is lost due to reduction of a 3-D scene to 2-D image and thus uniqueness of solution is not guaranteed. Therefore, in order to solve this problem we need to given certain additional information and to use it as a constraint.

When there is a peculiar texture on an object surface, a number of methods that effectively utilize its property have been proposed thus far. Gibson [1] noted texels which are constituent elements of texture and showed that under assumption that it distributes on object surface with equivalent density, the orientation of the object surface can be estimated using distortion of texel density on projected images.

Ohta et al. [2] extracted the vanishing point by formulating the relationship between area ratio of texels and distortion due to projection and found object surface orientation. These assume that texel structures are known in advance. However, in the case in which a texel structure cannot be specified, it is difficult to extract texels from a real image and error grows depending on the precision of extracted texels.

On the other hand, Kender calculated the orientation of object surface with parallel edges as clues using the property that a group of parallel lines on object surface are projected into a group of half-lines whose endpoint is one point (the vanishing point) on images.

Witkin [4] estimated surface orientation by a stochastic method, noticing directions of edge segments of texels and specifying the probability density distribution of edge directions on object surface in advance.

ISSN0882-1666/91/0011-0100$7.50/0

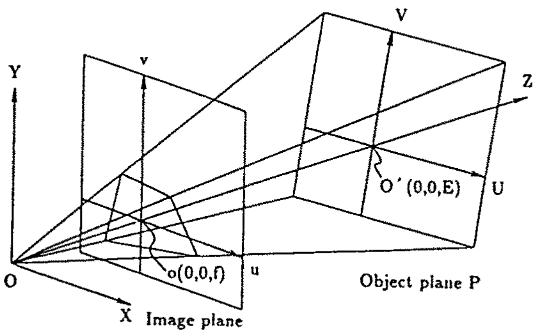

Fig. 1. The coordinate systems and the perspective projection.

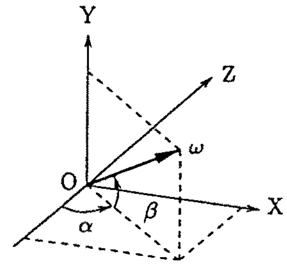

Fig. 2. The surface normal vector.

Further, Aloimonos [5] extended the assumption by Gibson and assumed that edge elements, constituent elements of texels on object surface, are distributed in uniform density and then formulated the relationship between change of density of sum of edge lengths in each local area in an image and surface orientation and extracted surface orientation.

Since these methods note edge elements, they can be applied to some extent to textures in which texel structures cannot be specified. However, in some images edge elements cannot be extracted correctly in some objective images, edges are extracted in locations which differ from the real ones, and/or valid edges may not exist. As stated, a method in which texture is represented by statistical features directly using gray levels is effective for textures in which clear boundary does not exist or ones without clear structures and those for which extracting edges is difficult. Methods based on statistical quantity are applied to image segmentation [8]. However, there is no example to find object surface using statistical features.

In this paper we consider a method in which we represent textures by statistics of gray levels and extract surface orientation using the statistical property. When a plane of uniform statistical property on object surface is projected on an image surface, statistical congruence is broken between local regions and some distortion arises. Description of the relationship between this distortion and surface orientation enables us to extract orientation of the surface. Here we use for this statistical property a difference statistic in which gray level difference is defined as a probability density function depending on distance and direction. We first assume that these statistics have the same density function in every local region on object surface and formulate the relation between the distortion of the difference statistics and surface orientation in local regions on an image under the perspective projection. Then we derive an algorithm for extracting surface orientation based on this formulation and examine its efficiency by experiments.

2. Geometric Relation Between Surface and Image Plane

2.1. Coordinate system and perspective projection

Consider the 3-D coordinate system *OXYZ*, as shown in Fig. 1, in which the origin *O* is the view point. Suppose that an image plane is the plane *ouv* perpendicular to the *Z* axis (vision axis) whose origin is $(0, 0, f)$. Let *E* be the distance to object surface *P* and the orthogonal coordinate system *O'UV* with $(0, 0, E)$ at the origin is settled on the plane *P* so that the *U* axis lies in the same plane (*OXZ* plane) as the *u* axis. Thus, the normal vector ω to the plane *P* can be uniquely determined by angles α and β, as illustrated in Fig. 2. Then we have $\omega = (\sin\alpha\cos\beta, \sin\beta\cos\alpha\cos\beta)$ and the equation of the plane *P* is given by

$$bcX + dY - ac(Z-E) = 0 \tag{1}$$

Here,

$$a=\cos\alpha,\ b=\sin\alpha,\ c=\cos\beta,\ d=\sin\beta$$

The problem of extracting surface orientation is equivalent to that of finding these angles α, β.

Letting $f = 1$ in the foregoing coordinate system, the relation between object surface $P(U, V)$ and an image plane (u, v) under the perspective projection is

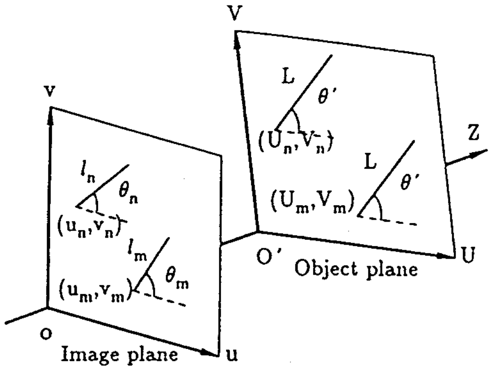

Fig. 3. The constraint conditions for the distance and direction on the image plane.

$$U=\frac{E(cu+bdv)}{ac-bcu-dv},\quad V=\frac{Eav}{ac-bcu-dv} \tag{2}$$

2.2. Relation between length of line segments and directions

When we project in perspective a line segment onto an image plane, lengths and directions change due to distortion caused by projection. In an object surface P for a line segment of length L and direction θ' whose endpoint is $\langle U, V\rangle$ and a line segment of length l and direction θ whose endpoint is (u, v) in the image plane after projection, the relation among L and l, θ and θ' is

$$\begin{aligned} L=&Eac/[(ac-bcu-dv)\{ac-bc(u+l\cos\theta)\\ &-d(v+l\sin\theta)\}\\ &\cdot[\{(c-adv)\cos\theta+d(b+au)\sin\theta\}^2\\ &+\{bv\cos\theta+(a-bu)\sin\theta\}^2]^{1/2}\cdot l] \end{aligned} \tag{3}$$

$$\theta'=\tan^{-1}\left[\frac{bv\cos\theta+(a-bu)\sin\theta}{(c-adv)\cos\theta+d(b+au)\sin\theta}\right] \tag{4}$$

2.3. Constraint on distance and direction in an image plane

Given a pair of parallel line segments of length L and direction θ' with two endpoints (U_m, V_m) and (U_n, V_n) on object surface P (endpoints on an image plane are (u_m, v_m) and (u_n, v_n), respectively), as shown in Fig. 3, generally we have $l_m \neq l_n$ and $\theta_m \neq \theta_n$ in the image plane after perspective projection. Then, from Eqs. (3) and (4), there is the following relationship between l_m and l_n and between θ_m and θ_n:

$$\begin{aligned} &[\{(c-adv_m)\cos\theta_m+d(b+au_m)\sin\theta_m\}^2\\ &\quad+\{bv_m\cos\theta_m+(a-bu_m)\sin\theta_m\}^2]^{1/2}\cdot l_m\\ &\quad\cdot[(ac-bcu_m-dv_m)\\ &\quad\cdot\{ac-bc(u_m+l_m\cos\theta_m)-d(v_m+l_m\sin\theta_m)\}]^{-1}\\ &=[\{(c-adv_n)\cos\theta_n+d(b+au_n)\sin\theta_n\}^2\\ &\quad+\{bv_n\cos\theta_n+(a-bu_n)\sin\theta_n\}^2]^{1/2}\cdot l_n\\ &\quad\cdot[(ac-bcu_n-dv_n)\\ &\quad\cdot\{ac-bc(u_n+l_n\cos\theta_n)-d(v_n+l_n\sin\theta_n)\}]^{-1} \end{aligned} \tag{5}$$

$$\begin{aligned} &\frac{bv_m\cos\theta_m+(a-bu_m)\sin\theta_m}{(c-adv_m)\cos\theta_m+d(b+au_m)\sin\theta_m}\\ &=\frac{bv_n\cos\theta_n+(a-bu_n)\sin\theta_n}{(c-adv_n)\cos\theta_n+d(b+au_n)\sin\theta_n} \end{aligned} \tag{6}$$

If such a pair of line segments in an image plane is extracted and l_m, l_n, θ_m, θ_n are obtained, we can find parameters α, β by combining Eqs. (5) and (6) for two pairs of line segments. However, in this paper we do not use structural information of texture such as a line segment but aim to estimate orientation directly from gray levels. Therefore, noticing difference statistics depending on distance and direction, we try to estimate α and β from the property of pairs of imaginary parallel line segments.

3. Extraction of Surface Orientation Using Difference Statistics

3.1. Orientation extracting algorithm

Difference statistics is the probability $P(K|l, \theta)$ that the absolute value of gray level difference from pixels which are apart from some pixel by a certain displacement (l, θ) is K. Since this depends on distance and direction, we can represent texture features statistically.

Assuming that the probability density function of difference statistics is equal in every local area in the object plane; for probability density functions in some gions m and n we have the relationship

$$P_m(K\mid L_m, \theta_m')=P_n(K\mid L_n, \theta_n') \tag{7}$$

when $L_m = L_n$ and $\theta_m' = \theta_n'$. If we project it in perspective onto an image plane, there arises some distortion in the difference statistics due to the distortion by projection. The statistical congruence is broken because of this and the relationship in Eq. (7) does not hold. However, for l_m and l_n,

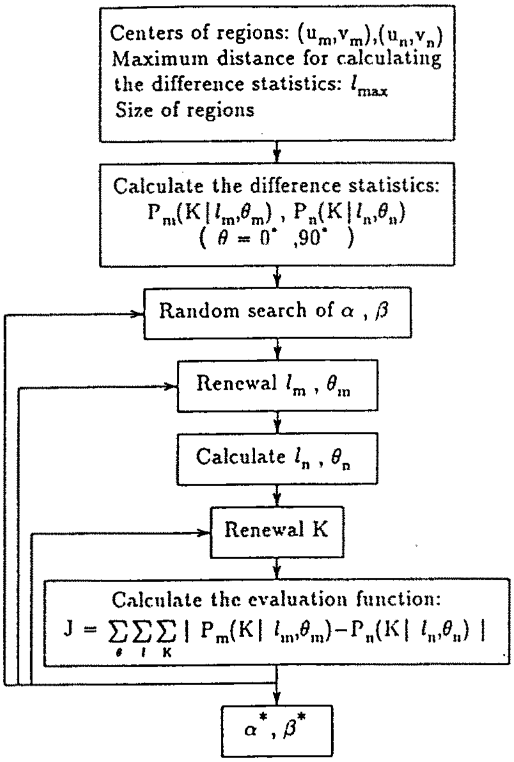

Fig. 4. The algorithm extracting a surface orientation.

and θ_n and θ_n satisfying Eqs. (5) and (6), we have

$$P_m(K \mid l_m, \theta_m)=P_n(K \mid l_n, \theta_n) \tag{8}$$

and density functions in the two regions in the image plane coincide. Thus, conversely, if we can find l_m and l_n, and θ_m and θ_n satisfying Eq. (8) using the density distributions of difference statistics $P_m(K \mid l_m, \theta_m)$, and $P_n(K \mid l_n, \theta_n)$ found from two local regions in the image plane, we can extract surface orientation. However, since difference statistics may be of various forms depending on textures, it is hard to find l_m, l_n, θ_m and θ_n satisfying Eqs. (5) and (6) in an analytic manner. So, in this paper, we introduce an evaluation function

$$J= \mid P_m(K \mid l_m, \theta_m)-P_n(K \mid l_n, \theta_n) \mid \tag{9}$$

to estimate the surface orientations α, β in a searching manner to minimize this evaluation function. That is, considering the difference statistics obtained from an image as feature patterns representing texture feature, we estimate the orientation by taking matching among feature patterns between regions by changing α and β.

3.2. Orientation extracting algorithm

(a) Outline of algorithm

Figure 4 shows the algorithm for extracting orientation. First, for an input image we settle the center of gravity of a region, size of a region, and the maximum value of distance by which difference statistics are computed. We find difference statistics of two regions $P_m(K \mid l_m, \theta_m)$, $P_n(K \mid l_n, \theta_n)$ with angular range $0 \leqq \theta < \pi$. Next, by giving α, β, l_m and θ_m, we compute corresponding l_n, θ_n from Eqs. (5) and (6) to compute J in Eq. (9). We estimate orientations α^*, β^* to minimize J while updating K, l, θ.

In order to apply this algorithm to real image data, we need correspondence of regions and interpolation of difference statistics due to the property of discrete image.

(b) Correspondence of local regions

Since an image consists of quantized pixels, we cannot calculate difference statistics for every direction θ when we measure difference statistics. We can obtain sufficient data with equal gap only for direction = 0°, 45°, 90°, and 135°. So, we devise settling the centers of gravity of regions as follows.

Since a line connecting centers of gravity of two regions on object surface is transformed also into a line after perspective projection, for direction after projection of the two lines that coincide in that direction we have $\theta = \theta_m = \theta_n$ in Eq. (5). That is, if we settle centers of gravity of two regions on lines of θ = 0°, 45°, 90°, 135° and combine Eqs. (5) and (6), we can condense it as follows:

$$\begin{aligned} &l_m \cdot [(ac-bcu_m-dv_m) \\ &\quad \cdot \{ac-bc(u_m+l_m\cos\theta_m)-d(v_m+l_m\sin\theta_m)\}]^{-1} \\ &= l_n \cdot [(ac-bcu_n-dv_n) \\ &\quad \cdot \{ac-bc(u_n+l_n\cos\theta_n)-d(v_n+l_n\sin\theta_n)\}]^{-1} \end{aligned} \tag{10}$$

Since it suffices to compute only in fixed directions, we can compute J only by updating the distance l_m. Here, we settle the four regions as shown in Fig. 5 and

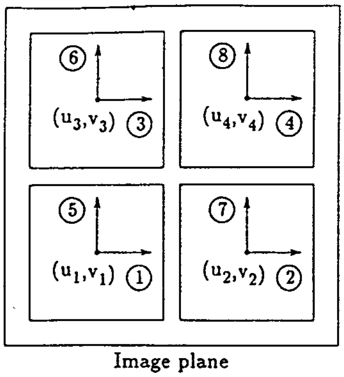

(1) ① $P_1(K|l_1,0^\circ)$ ⟷ ② $P_2(K|l_2,0^\circ)$
(2) ③ $P_3(K|l_3,0^\circ)$ ⟷ ④ $P_4(K|l_4,0^\circ)$
(3) ⑤ $P_1(K|l_1,90^\circ)$ ⟷ ⑥ $P_3(K|l_3,90^\circ)$
(4) ⑦ $P_2(K|l_2,90^\circ)$ ⟷ ⑧ $P_4(K|l_4,90^\circ)$

Fig. 5. The corresponding directions between local regions on an image.

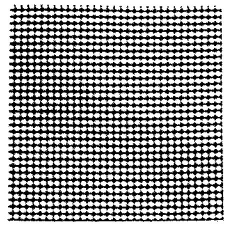

Fig. 6. The periodic image pattern.

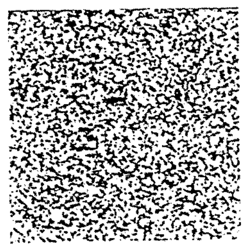

Fig. 7. The MRF texture image.

estimate the orientations α and β with $\theta = 0^\circ, 90^\circ$.

(c) Interpolation of distribution of difference statistics

The difference statistics $P(K|l,\theta)$ can only be computed in a discrete manner with respect to the distance l because an image is discrete. Thus, even if we choose l_m in Eq. (10) so as to be a computable value, it does not always imply that $P_n(K|l_n, \theta)$ for corresponding l_n becomes computable. So, we interpolated the difference statistics distribution $P(K|l, \theta)$ by a natural Spline function [9] with respect to the distance l.

(d) Search method

In order to find orientations α and β to minimize J, it suffices to compute J for every α and β in the range $-90^\circ \leq (\alpha, \beta) \leq 90^\circ$, but the problem is its computational complexity. So, in order to perform efficient search, we use the following search algorithm.

<Search algorithm>

(1) Choose 20 (α, β)s in the range $-30^\circ \leq \alpha, \beta \leq 30^\circ$ randomly and compute J.

(2) Let $(\alpha, \beta)_{min}$ that minimizes J be the central value and J_c be J at that time.

(3) Choose 20 (α, β) near the center value in the range $(\alpha, \beta)_{min} \pm 10^\circ$ randomly to compute J and let J_{min} be the minimum one of those J.

(4) If for J_{min} and J_c we have $J_{min} < J_c$, then let α and β for J_{min} be the center value $(\alpha, \beta)_{min}$ and then go back to (3).

If $J_{min} \geqq J_c$, then go back to (3) after reducing the search range by 1°. Here, note that we do not reduce the search range by more than ±2°.

(5) we terminate the search if $(\alpha, \beta)_{min}$ is not changed after the 10th iteration and the value of (α, β) at that time be the estimated value (α*, β*).

4. Application to Images

In order to verify the effectiveness of this method, we estimated orientations by applying this method to images generated by simulation and texture images which were taken by a CCD camera.

Table 1. Results of estimated orientations (1)

Periodic pattern		MRF texture	
true values α, β	estimated values α^*, β^*	true values α, β	estimated values α^*, β^*
10°, 10°	10°, 11°	10°, 10°	10°, 10°
20°, 0°	20°, 0°	20°, 0°	20°, 1°
		0°, 20°	−3°, 22°

Region centers: (100, 100), (100, 300), (300, 100), (300, 300)

Region size: 101 × 101

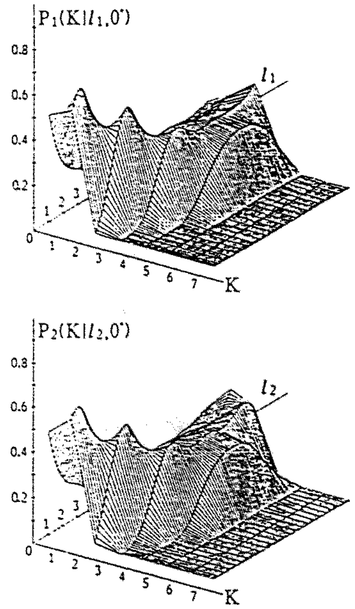

Fig. 8. An example of the gray-level difference statistics of the inclined image (α = β = 10°) of Fig. 6.

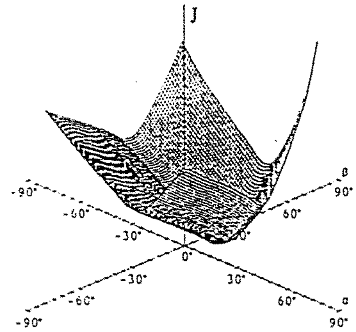

Fig. 9. The evaluation function of the inclined image (α = β = 10°) of Fig. 6.

4.1. Simulation images

Figure 6 is a periodic texture image using a sin function in which one cycle is 16 pixels and which has eight gray levels. Figure 7 is a texture generated by using the MRF model [8] with five gray levels. The size of the images is 512 × 512 pixels. We transformed them with the origin at the lower left corner and estimated the orientations α, β where region centers are (100, 100), (100, 300), (300, 300), the size of a local area is 101 × 101 pixels, the maximum length l_{max} in which difference statistics is computed. Figure 8 shows the difference statistics found for a periodic pattern when α = β = 10° and Fig. 9 shows the evaluation function and Table 1 is the estimation results. We obtained the results that the error is within ±1° for periodic patterns and it is ±3° for MRF textures. These errors are originated in that although textures have 2-D features, they are defined as features of representative points in a degenerated manner. Moreover, since we are required to interpolate data to deal with discrete images, some error arises from its estimation error. For MRF textures, it is not necessarily guaranteed that difference statistics have the same profile. In other

Table 2. Results of estimated orientations (2)

Region centers	Estimated values α^*, β^*	Region centers	Estimated values α^*, β^*
(100, 100), (150, 100) (100, 150), (150, 150)	11°, 7°	(100, 100), (300, 100) (100, 300), (300, 300)	10°, 11°
(100, 100), (200, 100) (100, 200), (200, 200)	9°, 10°	(100, 100), (350, 100) (100, 350), (350, 350)	10°, 10°
(100, 100), (250, 100) (100, 250), (250, 250)	8°, 11°		

True value: $\alpha=\beta=10°$, region size: 101×101

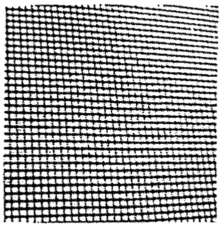

Fig. 10. Real texture image (1).

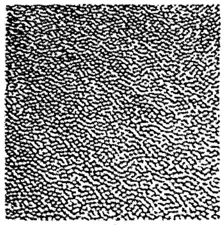

Fig. 12. Real texture image (3).

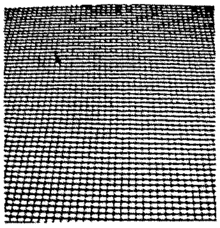

Fig. 11. Real texture image (2).

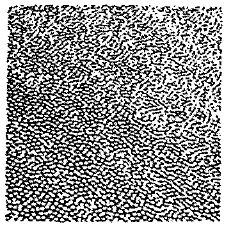

Fig. 13. Real texture image (4).

words, we can say that MRF textures are those objects for which there is no guarantee that the assumption in our method holds.

We also examined the influence when we changed region centers. Table 2 shows the result when we changed the region centers for an image with a periodic pattern with $\alpha = \beta = 10°$ (the size of the image is 50). In this case, error increases when we overlay regions. It is considered that this is because it was made unable to extract dis tortion due to projection sufficiently si the overlapped portion possesses a common statistical property.

4.2. Real images

Next, we applied our method to textu images taken by a CCD camera. The images were taken with size of 240 × 240 pixels

Table 3. Results of estimated orientations (3)

	True values α, β	Estimated values α^*, β^*
Fig. 10	20.9°, 20.2°	20°, 22°
Fig. 11	0.0°, 48.1°	0°, 47°
Fig. 12	18.0°, 24.2°	16°, 26°
Fig. 13	13.1°, 37.6°	7°, 38°

Region centers: (-69, -70), (41, -70), (-69, 40), (41, 40)
Region size: 81 × 81

and 256 gray levels and the center of the images are taken as the origin. Figures 10 through 13 are those images in which gray levels are made to be 8 by an equal-probability quantizing algorithm [6]. Table 3 includes the results when we estimated orientations where region centers are (-69, 70), (41, -70), (-69, 40) and (41, 40) and the size of regions is 81 × 81 pixels. Regions are estimated with error within ±2° except Fig. 13 in spite of worsened image due to fade. For Fig. 13 for which the error is large, if we estimate the orientation with the same region centers and region size 101 × 101, we obtained the results $\alpha = 13°$, $\beta = 37°$. It is considered that this is because the statistical feature is fully reflected in difference statistics by enlarging the region size. In addition to the problem concerning errors described in the previous section, it may be considered that since existing objects are input through a TV camera noise at signal level, quantization error and transformation error are overlaid.

In addition, in order to verify whether the search algorithm for optimal solutions is good or not for simulation images and real ones, we computed the minimum value of the evaluation function for all those images used this time. Then all of them coincided with optimal values found by this algorithm.

In this way, in spite of influence by various kinds of noise, it was verified that orientations in a texture image can be extracted sufficiently by this method using difference statistics.

5. Conclusions

This paper proposed a method for extracting orientation of object surface using statistical property of a texture image. In this method we use effectively gray levels of an image which were not considered previously. This enables us to avoid various problems in estimation and extraction of texel and edge extraction and to extract orientation of object surface using gray levels directly from gray level images.

However, the method can be applied only to a texture image whose difference statistics is uniform, and for other objects error according to the uniformity arises. Also, depending on the area in which statistics is measured, in some cases texture feature cannot be fully reflected. In the future, we need to clarify the class of texture for which difference statistics are uniform and to consider how a large area should be set according to texture.

REFERENCES

1. J. J. Gibson. The Perception of the Visual World. Houghton Mifflin, Boston (1950).
2. Y. Ohta, K. Maenobu, and T. Sakai. A method for obtaining surface orientation from perspectively projected texture. Proc. of Computer Vision Workshop of IPS of Japan, 16-2, pp. 1-8 (1982).
3. J. R. Kender. Shape from texture: An aggregation transform that maps a class of textures into surface orientation. Proc. 6th IJCAI, pp. 475-480 (1979).
4. A. P. Witkin. Recovering surface shape and orientation from texture. Artif. Intell., 17, pp. 17-45 (1981).
5. J. Aloimonos. Shape from texture. Biol. Cybern., 58, pp. 345-360 (1988).
6. R. M. Haralick, K. Shanmugam, and I. Dinstein. Textural features for image classification. IEEE Trans. Syst., Man & Cybern., SMC-3, 6, pp. 610-621 (1973).
7. J. S. Weszka, C. R. Dyer, and A. Rosenfeld. A comparative study of texture measures for terrain classification. IEEE Trans. Syst., Man & Cybern., SMC-6, 4, pp. 269-285 (1976).
8. S. Geman and D. Geman. Stochastic relaxation, Gibbs distributions, and the Bayesian restoration of images. IEEE Trans. Pattern Anal. & Machine Intell., PAMI-6, 6, pp. 721-741 (1984).
9. N. Takemoto and M. Ara. Numerical Computation by C. Asakura Publ., pp. 86-104 (1987).

AUTHORS (from left to right)

   

Mutsuhiro Terauchi graduated in 1984 from the Department of Mechanical Engineering, Faculty of Engineering, Kansai University, where he obtained a Master's degree in 1986. Currently, he is engaged in research on computer vision and image understanding. He is a member of AVIRG; IEEE; and the Information Processing Society of Japan.

Hidegi Matsushima graduated in 1988 from Group 2 (Electrical Engineering), Faculty of Engineering, Hiroshima University, and in 1990 obtained a Master's degree from there in Information and Computer Science. He then joined NTT Data Communication Corp. As a student, he was engaged in research on computer vision. He is a member of the Japanese Human Engineering Society.

Toshio Tsuji obtained a Master's degree from the Faculty of tngineering, Hiroshima University, in System Engineering in 1985 and later obtained a Dr. of Eng. degree. He became a Research Associate in 1985 and has remained in that position. He is engaged in research on somatological engineering, robot engineering, and man-machine system. He is a member of the Society of Measurement and Automatic Control; Institute for Electrical Engineers, Japan; Robot Society; Japanese Human Engineering Society; and IEEE.

Koji Ito obtained a Master's degree in 1969 from Nagoya University, where in 1970 he became a Research Associate in automatic control. He has a Ph.D. He has been an Associate Professor of Group 2 (Electrical Engineering) of the Faculty of Engineering, Hiroshima University, since 1979. He is engaged in research on somatological system analysis, robotics, and man-machine interface. He is a member of the Society of Measurement and Automatic Control; Institute for Electrical Engineers, Japan; Robot Society; Japanese ME Society; and IEEE.